

# Fracture and fatigue performance of textile commingled yarn composites

M. D. GILCHRIST

*Department of Mechanical Engineering, University College Dublin, Belfield, Dublin 4, Ireland*

N. SVENSSON

*Pelmatic Consulting Engineers, F O Petersons gata 28, S-42131, Västra Frölunda, Sweden*

R. SHISHOO

*Swedish Institute for Fibre and Polymer Research, PO Box 104, S-43122 Mölndal, Sweden*

The response to mechanical loads of unidirectional commingled warp knitted and woven glass fibre reinforced polyethylene terephthalate laminates has been characterized. The mechanical properties of the two materials were determined under tension, in-plane shear and flexure. The flexural fatigue properties were determined for the woven laminates by means of three-point bending tests with a loading ratio of  $R = 0.1$  at stress levels of 50–90% of the ultimate static strength. The Mode I, Mode II and mixed mode (Mode I:II ratios 4:1, 1:1 and 1:4) interlaminar fracture toughnesses of the laminates were determined by means of the double cantilever beam and mixed mode bending tests, respectively. The main fractographic features, as determined by a scanning electron microscopy examination, of the Mode I dominated failures were a brittle matrix failure and larger amounts of fibre pull-out. As the Mode II loading component increased, the amount of fibre pull-out was reduced and the features of the matrix appeared to be more sheared. Cusps were found on the fracture surfaces of specimens tested in pure Mode II and mixed mode I:II = 1:4. Cusps are normally not found in thermoplastic matrix composites. © 1998 Kluwer Academic Publishers

## 1. Introduction

The interest in using textile thermoplastic composite materials has increased substantially within the past decade. This is due to a number of reasons [1–5]:

1. it is much easier to recycle thermoplastic matrix composites than those based on thermoset resins;
2. the shelf life of a thermoplastic matrix prepreg is almost unlimited and there are no requirements for storage at sub-zero temperatures;
3. there is large potential for fast automated manufacturing (processes similar to compression moulding and diaphragm moulding of glass mat thermoplastic (GMT) materials);
4. thermoplastic composites may be post-shaped and welded;
5. a thermoplastic matrix has a higher elongation at fracture and a higher resistance to crack propagation than ordinary thermoset matrices; and
6. textile processes, such as weaving, braiding and knitting, enable faster fabrication and tailoring of the fibre architecture of preforms than are currently offered by conventional and prepreg techniques.

Commingled yarns, i.e. yarns in which the reinforcing fibres are intimately mixed with spun thermoplastic matrix fibres, are a novel form of intermediate materials suitable for manufacturing load carrying thermoplastic composites. As the yarns are flexible,

they can be used in any textile process. Consequently drapable and highly conformable fabrics and structures may be produced. A wide variety of fibre–matrix combinations are available in commingled form [6]. Production cycle times range from below 1 min to several hours depending on the matrix material as well as on the required pressure and processing temperature. Process control is crucial as overheating degrades the matrix material and reduces the final composite properties. A pressure of 0.3–1.5 MPa is required for good consolidation in a reasonable time and for semicrystalline polymer matrices the cooling should preferably be rapid to prevent the formation and growth of large spherulites that reduce the fracture toughness of the composite. Pressure applied during cooling hinders deconsolidation, which deteriorates the mechanical properties of the composite.

The present work describes the mechanical response under tension, in-plane shear and flexure of thermoplastic laminates manufactured from warp knitted and woven fabrics. The flexural fatigue behaviour was characterized together with the resistance to interlaminar crack propagation in Mode I, Mode II and mixed modes (I:II) 4:1, 1:1 and 1:4. A scanning electron microscopy (SEM) analysis was conducted to elucidate the fracture processes and the laminate quality.

## 2. Experimental procedure

The constituents of the commingled yarn used were glass fibres and polyethylene terephthalate (GF–PET) fibres. The glass fibre volume fraction in the yarns was 48% and the yarns were produced by means of air-jet texturizing. The laminates were manufactured from woven and unidirectional warp knitted fabrics. The woven fabric was designed with the main fraction (five-sixths) of the fibres being aligned in the warp direction. The warp knitted fabric was unidirectional and the commingled yarns were held together by a thin PET yarn, Fig. 1.

The formability, i.e. bending and shear properties, and the compression behaviour of the two fabrics were evaluated [7] by means of the Kawabata evaluation system (KES), which is an established method for the characterization of mechanical and surface properties of sheet materials.

The fabrics were cut and stacked to produce unidirectional and cross-ply laminates. Twenty layers were used for the warp knitted fabric and 12 layers for the woven fabric. Steel guide bars were used to obtain a uniform laminate thickness. The consolidation pressure was provided by compacting the fabric stacks from the uncompressed thickness of about 12 mm to the target thickness of 3 mm. The warp knitted fabrics were more difficult to compress and the warp knitted cross-ply laminates consequently resulted in a thickness of 4 mm. A Nylon 6 film with a thickness of 50  $\mu\text{m}$  and coated with release agent was used to induce starter cracks in the laminates that were subsequently used for fracture toughness testing.

The laminates were compression moulded in a hydraulic press between steel platens. The mould was heated to 210 °C within 20 min and the consolidation time was also 20 min. The cooling rate was 21 °C  $\text{min}^{-1}$ . Pressure was applied during heating as well as during cooling. The glass fibre volume fraction for the laminates was determined by matrix burn-off and was determined to be 48.1%. The quality of the laminates was examined by observing polished cross-sections in an optical microscope. The glass transition temperature,  $T_g$ , of the PET matrix was determined

by means of dynamical mechanical thermal analysis (DMTA) to be 75.8 °C. A number of the woven laminates were annealed for 3 h at 110 °C to investigate if any differences in fracture properties could be observed as a result of the different thermal histories and hence different microstructures. This is discussed further in the following section.

The warp and weft direction tensile properties of the two different kinds of laminates were determined in accordance with ASTM D3039. The in-plane shear behaviour was determined following ASTM D3518. The static flexural properties of the laminates were determined in the warp and weft directions using a three-point bend test, ASTM D790M, with a span to thickness ratio of 16:1.

For the fatigue tests, three-point bending with a span to thickness ratio of 32:1 was used. The woven material was characterized in fatigue. A loading ratio of  $R = 0.1$  (the loading ratio defines the ratio of minimum to maximum load during a complete fatigue cycle) was used at five different load levels, i.e. 50, 60, 70, 80 and 90% of the static flexure failure load. At least three specimens were tested at each load level.

The fracture mechanics specimens were cut using a band saw and the edges of the specimens were polished and coated with typewriter correction fluid and the crack tip was marked on the edges of the specimens. The specimen dimensions were in accordance with the double cantilever beam (DCB) test, ASTM D5528. The Mode I tests were carried out by means of the DCB test. Fore pure Mode II tests and mixed modes (Mode I:II loading ratio) 4:1, 1:1 and 1:4 tests the modified mixed mode bending (MMB) geometry [8–10] was used. An investigation of the fracture surfaces was carried out by means of a Jeol scanning electron microscope and the fracture surfaces were sputter coated with gold prior to SEM examination.

## 3. Results and discussion

It is important to note that the results presented in the following sections are unique to these particular fibre

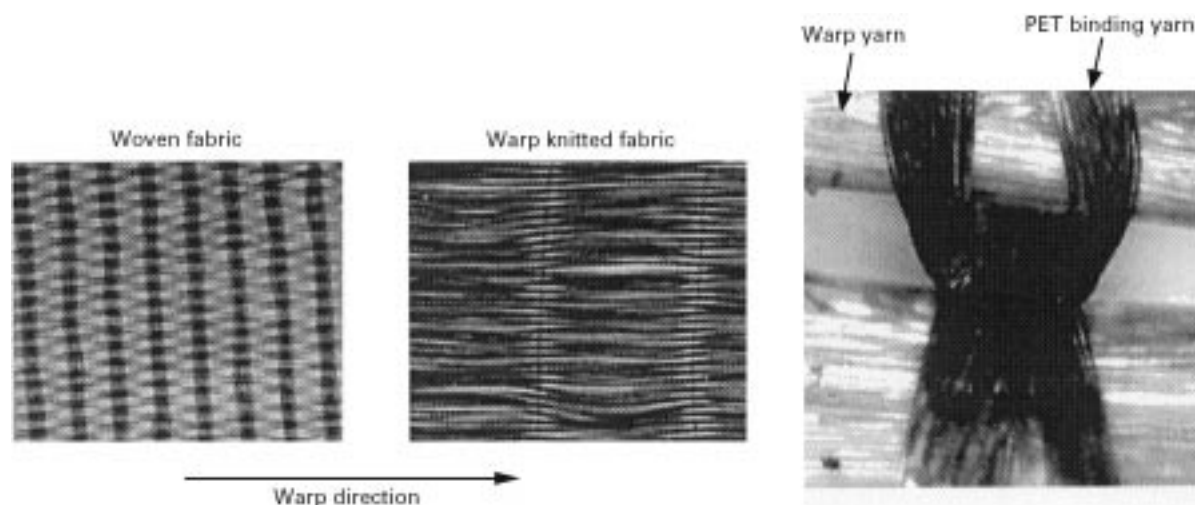


Figure 1 The two commingled yarn fabrics used for the fabrication of laminates. To the left is the woven fabric, in the middle the warp knitted fabric and to the right an optical micrograph of the PET binding yarn that holds the warp yarn together in the warp knitted fabric.

architectures and therefore cannot be generalized for all other woven or warp knitted composites.

The two fibre architectures that had been used made the fabrics very drapable, especially in the weft direction. Consequently they were difficult to handle and align and some variations in fibre angles between the plies in the laminates were inevitable. Due to the high draw ratio required for spinning the matrix fibres these are highly aligned and additional fibre misalignment in the composites may have been caused by contraction of these matrix fibres on heating. The crimp (i.e. the undulation of the warp and weft fibres) in the woven laminates was responsible for the large resin pockets in the material, especially in the cross-over areas between the warp and weft bundles. The fibre distribution was good outside the resin pockets. The reinforcing fibres in the warp knitted fabrics were non-crimped and there were fewer and smaller resin pockets than in the woven laminates. Cracks were occasionally seen in and between fibre bundles in both types of laminates. Very few voids were seen in the matrix. Similar observations in woven commingled GF-PET laminates have been made by Ye and Friedrich [11] who also reported large amounts of small voids in the resin rich regions between the warp and weft bundles in woven GF-PET laminates and these were caused by shrinkage upon crystallization. Angles between fibre bundles promoted the formation of voids. Shonaike *et al.* [12] examined commingled GF-PET composites and noted that the crystallinity of the matrix was not affected by different holding times during compression moulding. At short consolidation times many voids were present whereas at consolidation times  $>5$  min the impregnation was complete without any voids. Neither the melting temperature nor the crystallization temperature of the composite was affected by the holding time during consolidation. The fibre-matrix adhesion in the present material system was poor as can be seen from the very clean glass fibres in Fig. 2, which is a micrograph from a woven mixed mode 1:1 fracture specimen.

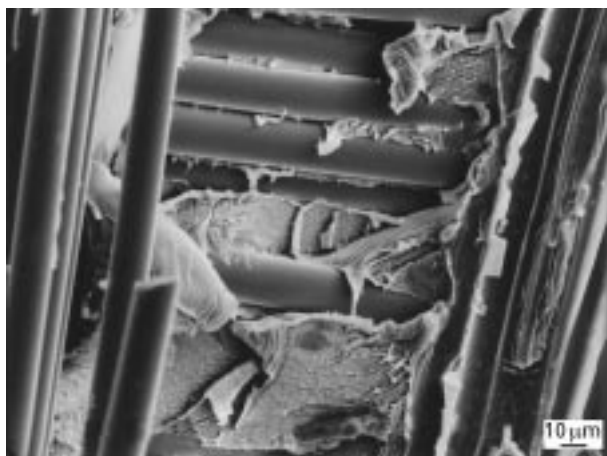


Figure 2 Clean fibres on the fracture surface of a mixed mode 1:1 woven sample showing the poor adhesion between the fibres and the matrix (i.e. clean fibres). The induced global crack propagation direction is from the bottom to the top in the micrograph. Tilt angle  $30^\circ$ .

### 3.1. Tension and in-plane shear

Neither matrix cracking nor fibre fracture was observed prior to failure during warp direction tensile tests. Failure of these test specimens occurred very suddenly although the specimens did not shatter dramatically in the fashion of unidirectional prepreg laminates. A limited amount of longitudinal splitting occurred at failure in the warp knitted laminates. A small stiffening was apparent for both materials as the load increased from zero and this was attributed to reorientation of the misaligned glass fibres during loading. The warp knitted laminates were slightly stiffer than the woven laminates and both materials were comparably strong, Table I. In the weft direction the woven laminates were stiffer and stronger due to the reinforcing glass fibres present in the weft yarns. The transverse tensile failures of the warp knitted laminates resembled those of a pure thermoplastic with an extensive amount of plastic deformation while the woven laminates were almost fully elastic until failure in both the warp and weft directions. Extensive delaminations and fibre pull-out took place during failure.

The experimental values of the tensile properties were slightly lower than those predicted by the rule of mixtures [7]. These deviations were probably caused by the poor fibre-matrix adhesion and the fibre misalignment during stacking and manufacturing. The modulus of the woven laminates in the warp direction was lower than that of the warp knitted due to the smaller fraction of glass fibres in this direction and also due to the crimp in the fibre architecture.

The in-plane shear moduli for the two materials were similar although the woven laminates had a marginally greater in-plane shear strength (calculated at the maximum load) than the warp knitted laminates. The shear failures of both materials were similar and involved large amounts of stress whitening. The scatter in the shear properties was larger for the warp knitted laminates and the fibre misalignment was believed to be responsible for this.

### 3.2. Flexure

In the static flexural tests the warp knitted laminates were stronger and stiffer than the woven laminates in the warp direction while the woven laminates were stronger and stiffer when tested in the weft direction,

TABLE I The mechanical properties of the two different GF-PET laminates

Mechanical property	Woven	Warp knitted
Warp direction		
Tensile modulus, GPa	22.9	28.2
Tensile strength, MPa	510.4	486.6
Weft direction		
Tensile modulus, GPa	6.9	3.5
Tensile strength, MPa	130.9	6.6
In-plane shear		
Modulus, GPa	4.4	4.3
Strength, MPa	98.7	88.4

Table II. This latter effect was again due to the reinforcing glass fibres in the weft yarns of the woven laminates. The values of the moduli were consistently and significantly higher in flexure than in tension. The flexural modulus is dependent not only upon the fibre properties, fibre angles and fibre volume fraction but also on the stacking sequence. In all cases failures initiated on the compression side close to, or under, the loading pin. Cracks and limited delaminations propagated from the initial damage until final rupture of the specimen. Cracks were also seen to propagate along adjacent weft bundles in the woven laminates. The damage on the tensile face occurred in the form of fractures within the glass fibre yarns and cracking of the matrix between the yarns. This can be seen in the micrographs of the damage that developed on the tensile face of a warp knitted specimen, Fig. 3.

The warp knitted laminates withstood a higher load before failure but exhibited a larger drop in their load bearing capabilities when compared to the woven laminates. The tests were stopped manually after the load drop because the toughness of the materials prevented the specimens from fracturing before the specimens folded in between the supports of the three-point bending jig.

The cross-ply laminates were also tested in three-point bending. No differences in the fracture behaviour was seen when compared to the unidirectional

laminates. The flexural modulus of the warp knitted laminates was lower than for the woven laminates, which was contrary to what had been expected. This could be explained by the fact that the warp knitted cross-ply laminates were slightly thicker due to compaction problems during the compression moulding of the different laminates. This meant that the span to thickness ratio for the specimens was only 12:1 and consequently a significant amount of shear loading was present. Some few interlaminar cracks were seen during the tests. The values for the warp knitted cross-ply laminates in Table II are therefore not representative for pure flexure of the material.

Fibre fracture on the tensile face was the anticipated mode of failure for all the flexural tests and initially it was believed that the failures occurred due to a combination of tension and shear even though a span to thickness ratio of 16:1, as recommended in the ASTM standard, was used. However, the majority of the results available in the literature [13,14] do describe flexural failures initiating in the matrix on the compression face even at span to thickness ratios higher than 16:1. Static three-point bending tests of woven specimens utilizing a span to thickness ratio of 32:1 were carried out in conjunction with the fatigue tests and these failures also initiated in compression. No difference in strengths or moduli was observed between the two different span to thickness ratios. The direct strain on the tensile face, as measured experimentally using strain gauges, was 1.2% at the initiation of the compression damage. Hence it was believed that the compression strength of the matrix limited the flexural performance of the laminates. Together with the previously discussed observations available in the literature, it appears reasonable to suggest that this might be the general case for many commingled thermoplastic matrix laminates, and not only for this particular polymer matrix system.

The material used in the present work exhibited a poor fibre–matrix adhesion, which might partly explain the fact that mechanical properties were lower than expected. The manufacturing process parameters for the material have not yet been optimized. Observations of a good quality fibre–matrix bond in commingled GF–PET composites were made by Ye and Friedrich [11] and Shonaike *et al.* [12]. One way to improve the adhesion between the reinforcing fibres and the matrix is by plasma treatment. Jang and Kim [15] improved the flexural strength and the interlaminar shear strength of co-woven carbon fibre–polyether ether ketone (CF–PEEK) by 52 and 16%, respectively, by treating the fabric for 3 min with a low temperature oxygen plasma treatment prior to compression moulding.

TABLE II The flexural properties of the unidirectional and warp knitted laminates

	Woven	Warp knitted
Warp direction		
Flexural modulus, GPa	29.0	35.0
Flexural strength, MPa	493.6	747.2
Weft direction		
Flexural modulus, GPa	10.7	4.6
Flexural strength, MPa	214.0	24.7
Cross-ply		
Flexural modulus, GPa	21.2	17.4
Flexural strength, MPa	318.8	323.4

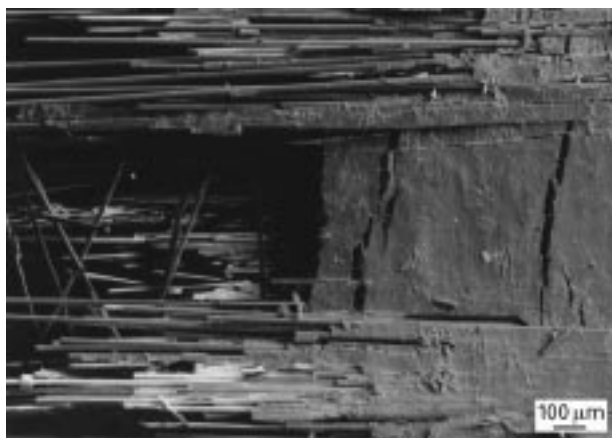


Figure 3 The tensile failure of a warp knitted three-point bending specimen. The glass fibre yarns hold together during the fracture. Cracks in the matrix are seen (to the right) between the glass fibre bundles.

### 3.3. Fracture

There was no visible difference between the Mode I fracture behaviour of the woven and the warp knitted laminates. Unstable slip–stick crack growth occurred in about one-half of the specimens. Non-linearities were recorded in the load–displacement curve before the maximum load was reached. A large amount of

fibre pull-out was seen during testing and this was responsible for both the resistance curve effect in the fracture toughness and the unstable crack growth. In the woven laminates the crack followed the undulation of the warp yarns as the cracks propagated from the end of the non-adhesive insert, Fig. 4.

The initiation values of fracture toughness were calculated at the point where the load–deflection curve deviated from linearity as shown schematically in Fig. 5. The propagation values of fracture toughness were calculated from the conditions of steady state crack growth. No significant difference was detected between the toughness of the annealed woven laminate and those of the ordinary woven laminate. The fracture toughness of the warp knitted laminates was lower than for the woven laminates and this was due to the weft yarns in the woven laminates, which made interlaminar crack propagation more difficult. The scatter in the fracture toughness data was greater for the mixed mode fractures in the cases of all three materials.

The fractographic examination of the Mode I fracture specimens revealed that the most dominant surface characteristic was fibre pull-out. Fig. 6 shows a large amount of fibre pull-out that occurred just ahead of the non-adhesive insert in a warp knitted



Figure 4 Fibre bridging during a Mode I test. The crack front is seen to be slightly bent out of plane and crack propagation followed the undulated paths of the warp yarns.

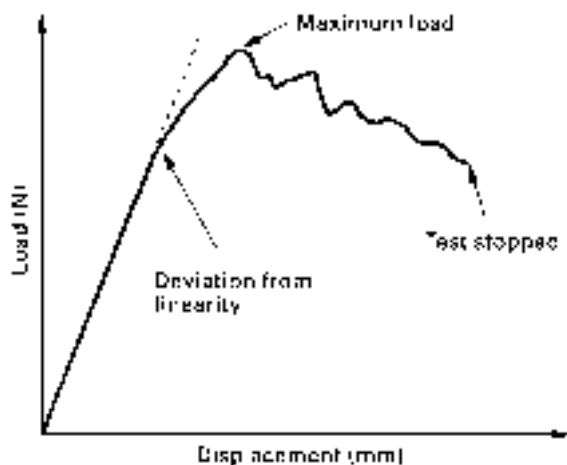


Figure 5 The schematic load–displacement curve of a double cantilever beam (DCB) test. The fracture toughness initiation values were calculated from the conditions at the onset of non-linearity.

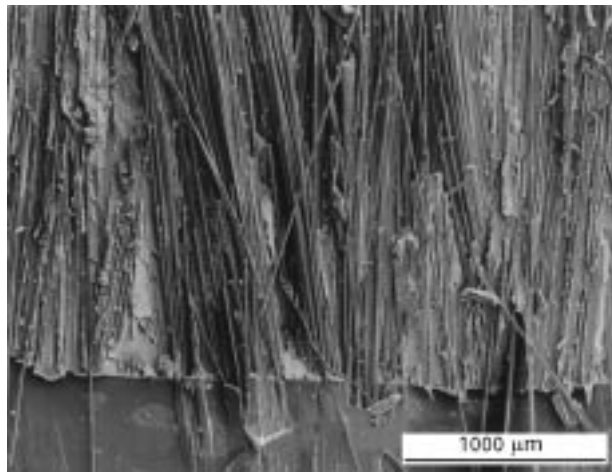


Figure 6 Extensive fibre pull-out ahead of the Nylon 6 insert of a warp knitted Mode I specimen. Some of the pulled out fibres extended back into the insert area. The induced global crack propagation direction is from the bottom to the top in the micrograph. Tilt angle 10°.

specimen. Some of the pulled out fibres can be seen to extend back into the insert area and this most likely contributed to the relatively high values of crack initiation energies. The amount of fibre pull-out was larger on the fracture surface of the warp knitted specimens and pull-out mainly occurred in bundles. In the woven laminates, on the other hand, the weft yarns limited the pull-out of fibres and yarns in the warp direction. The fibre pull-out was promoted by the poor strength of the fibre–matrix interface and the misalignment of the reinforcing fibres.

Crack propagation in the Mode II tests was more stable than in the Mode I tests. Fig. 7 shows a photograph of a warp knitted Mode II fracture surface. To the left is the area of the non-adhesive insert. The crack propagated from the end of the insert in a Mode II manner. The Mode II fracture surface is resin dominated with little fibre pull-out; this is the reason for the relatively smooth and light appearance of the fracture surface in this region. The crack front is curved and this curvature is due to differing stress states across the width of the specimen with plane stress conditions being present at the edges and plane strain in the centre [16]. The right part of the specimen, which is where the specimen was broken up manually, shows the appearance of a Mode I dominated fracture with fibre pull-out being present in the form of both bundles and yarns.

In brittle thermoset matrix composites, cusps are the main Mode II fracture surface characteristic. Cusp formation in thermoplastic matrix composites has been seldom observed due to the inherent ductility of most thermoplastic polymer matrices. Ye and Friedrich [11] have reported the formation of slanted cracks on the edge of commingled GF–PET specimens during Mode II testing. In the present work on both the woven and warp knitted laminates, comparatively many cusps were observed on the Mode II fracture surfaces, Fig. 8. The formation of cusps has been attributed to a brittle failure of the matrix [17–21] and can be described as the coalescence of

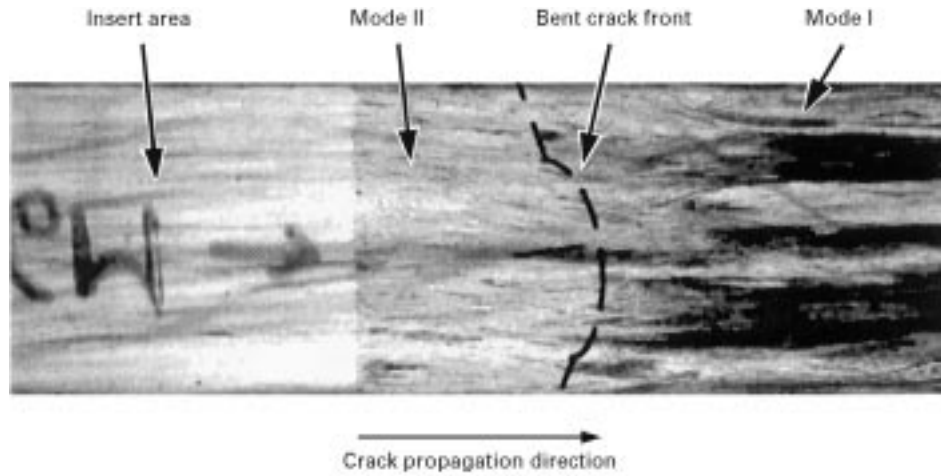


Figure 7 A photograph of a backlit warp knitted Mode II specimen. To the left is the end of the insert. The crack has propagated in Mode II, which has a bright matrix dominated appearance. The crack front is curved (shown by the dashed line). To the right is the area where the sample has been broken up manually by hand, i.e. crack propagation in a Mode I dominated manner.

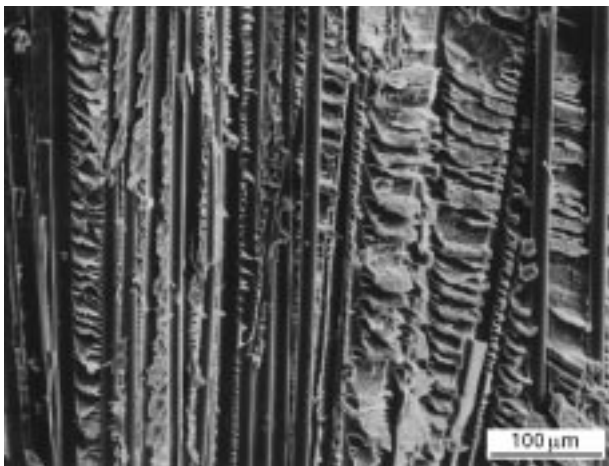


Figure 8 Rows of cusps evident between fibres on a Mode II fracture surface of a woven laminate. The induced global crack propagation direction is from the bottom to the top in the micrograph. Tilt angle 30°.

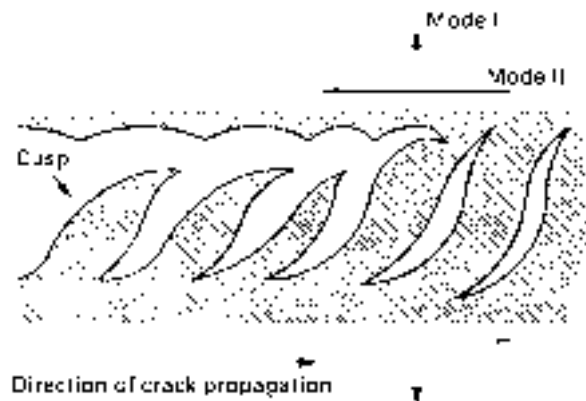


Figure 9 The formation of cusps as the coalescence of brittle microcracks ahead of the crack tip (interlaminar tensile, Mode I, and shear, Mode II, stresses; after Piggot [22]).

brittle microcracks that form perpendicular to the resolved principal stresses just ahead of the crack tip, as shown schematically in Fig. 9. The angle of the cusps theoretically vary with the mixed mode loading ratio, from 0° for pure Mode I to 45° for pure Mode II.

The presence of cusps indicates that this PET matrix failed in a brittle manner; this was also supported by the appearance of the matrix failure in Mode I, Fig. 10. Shear deformation of the matrix was also seen in Mode II dominated fractures, Fig. 11, but this was not as extensive as in previous work on other semi-crystalline thermoplastic matrix composites, such as CF-PEEK [23, 24].

Due to the relatively thick non-adhesive inserts used (i.e. 50 μm), matrix pockets were seen at the end of the inserts and these might also have increased the initiation fracture toughness of the laminates.

Difficulties were encountered when using the mixed mode bonding (MMB) jig for the mixed mode fracture tests on these relatively highly compliant material systems. Large deflections were present due to the tough matrix and the relatively low modulus glass

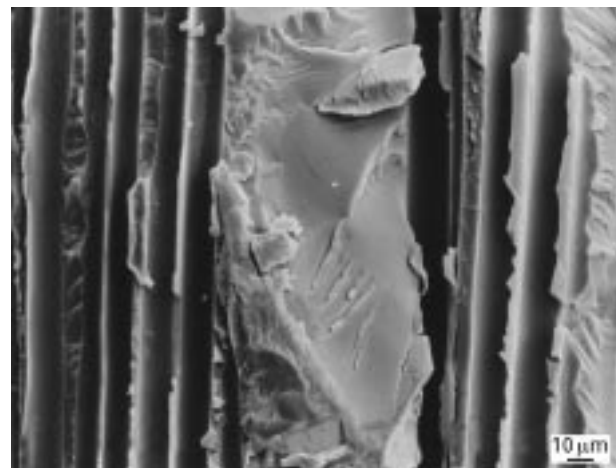


Figure 10 Tensile brittle matrix failure of a Mode I fracture surface of a warp knitted specimen. The induced global crack propagation direction is from the bottom to the top in the micrograph. Tilt angle 0°.

fibres. This resulted in the loading lever coming in contact with either the end of the specimen or the base of the jig although it did not affect the measurement of initiation and propagation values of fracture toughness. The jig has since been modified to handle such

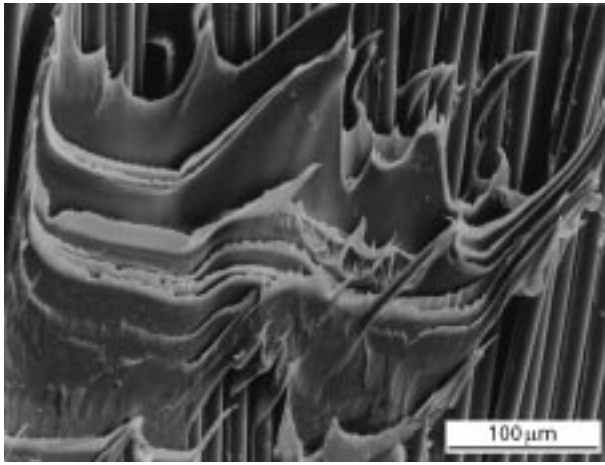


Figure 11 Matrix shear deformation on the surface of a woven Mode II fracture specimen. The induced global crack propagation direction is from the bottom to the top in the micrograph. Tilt angle 30°.

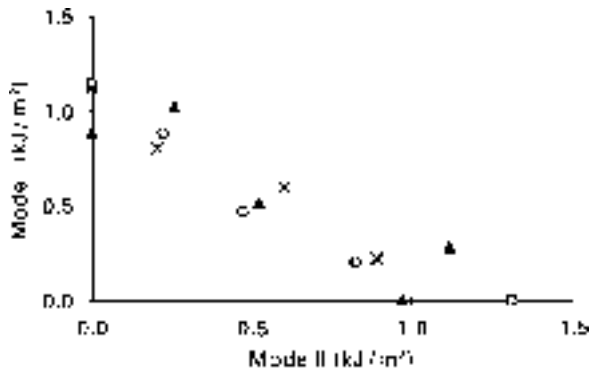


Figure 12 The experimentally determined initiation fracture toughness values for the three different material: (▲) warp knitted; (×) woven; (□) woven, annealed.

large deflections. Stable mixed mode crack growth was seen in most cases for both the warp knitted and woven laminates. Figs 12 and 13 show the experimentally determined failure loci for the three different materials in terms of both initiation and propagation fracture energies.

The mixed mode 4:1 fracture surfaces had an appearance that was similar to the Mode I fracture surfaces displaying both fibre pull-out and brittle, featureless matrix failure. Fig. 14 shows the area around the insert in a woven specimen tested at mixed mode 1:1. In the micrograph it is seen that the insert in this particular laminate ended in a weft bundle (running from left to right in the micrograph) that may have affected the crack initiation in this particular sample. The matrix is featureless and there are fibre imprints and some pulled-out fibres. The end of the non-adhesive insert is seen to be wavy due to the underlying glass fibre warp yarns.

Cusps were also found in the Mode II dominated mixed modes, Fig. 15. However, the amount of cusps was smaller than for pure Mode II. Compared to brittle epoxy matrix composites, cusps in the GF-PET material system were very rare and not as well defined, i.e. the cusps varied in size and appearance (compare

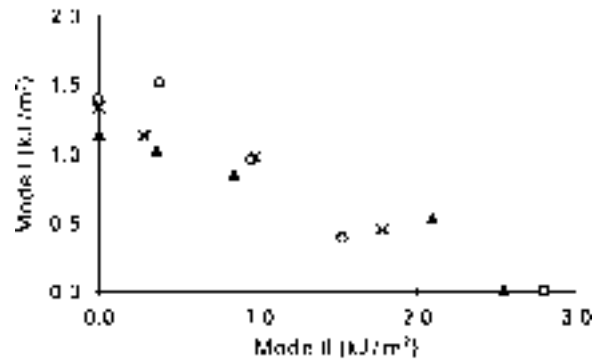


Figure 13 The experimentally determined propagation fracture toughness values for the three different material: (▲) warp knitted; (×) woven; (□) woven, annealed.

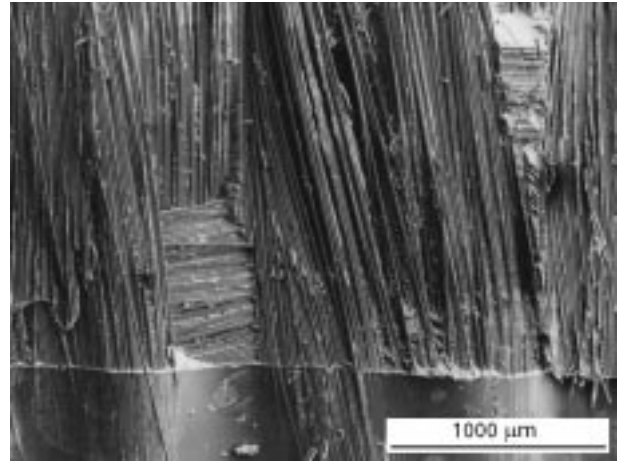


Figure 14 The area around the insert of an annealed woven specimen at low magnification. The crack has propagated in mixed mode 1:1. A slight waviness of the insert is seen as well as a large resin pocket (upper right corner). The induced global crack propagation direction is from the bottom to the top in the micrograph. Tilt angle 30°.

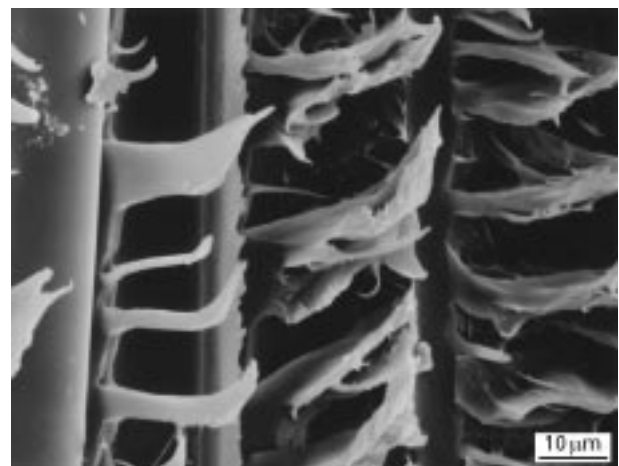


Figure 15 Small cusps with the tip bent over in the global crack propagation direction as seen on a mixed mode 1:4 fracture surface in an annealed woven specimen. The induced global crack propagation direction is from the bottom to the top in the micrograph. Tilt angle 30°.

Figs 8 and 15). The cusps in the different fracture modes also stood more upright (i.e. the cusp angle was larger) than the cusps that have been previously observed in epoxy matrices [21,25].

### 3.4. Fatigue

The fatigue performance of composites is important in structural applications where the material is subjected to cyclic loadings or deformations. In the presence of macroscopic defects or stress concentrations cracks will initiate and grow. Macroscopically the crack growth can often be described by a power-law type relationship. However, this crack growth will be more complicated when, for example, textile reinforcements are used as Hoffman and Wang [26] have observed in tests on chopped E-glass composites where the glass fibres were knitted together with continuous PET yarns. The notched specimens were loaded in tension and the typical fatigue crack propagation was characterized by “acceleration, retardation and deceleration” caused by the development of damage zones in the complex composite microstructure. The authors concluded that the knitting PET fibres contributed to the crack growth resistance by the introduction of elaborate failure mechanisms.

Information on the fatigue performance of continuous fibre reinforced engineering thermoplastics is very scarce in the literature. Gauthier *et al.* [27] examined the interlaminar fracture and fatigue performance of unidirectional GF-PET compression moulded at different temperatures (270 and 300 °C) and with different cooling rates (8 and 60 °C min<sup>-1</sup>). A brittle behaviour was observed for the slowly cooled specimens while the rapidly cooled specimens exhibited more ductile failures. The optimum toughness was obtained for low moulding temperatures and high cooling rates. The fatigue behaviour was assessed using a criterion based on a 10% decrease in flexural modulus and a typical S-N curve can be seen in Fig. 16. The authors also reported that for the specimens that had been moulded at the higher temperature, i.e. 300 °C, the improved wetting and interface strength limited the fatigue behaviour and energy dissipation. Fig. 17 shows the fatigue response of unidirectional continuous fibre and discontinuous fibre Kevlar 49/J-2 (J-2 is an amorphous polyamide copolymer) composites as determined by Okine *et al.* [28]. The discontinuous fibre composites (fibre lengths of 25–150 mm and an orientation with 85% of the fibres within the ± 5° directions) behaved in a similar manner to the continuous fibre composites.

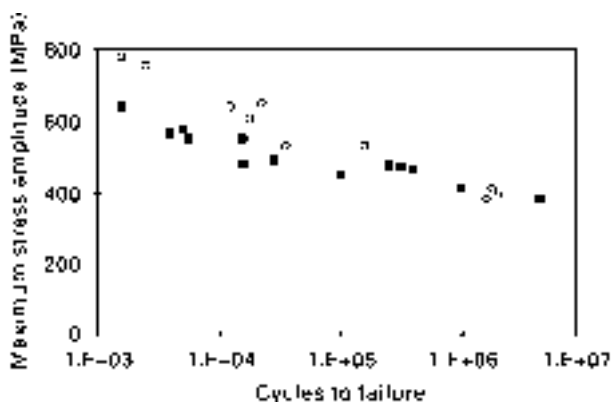


Figure 16 The S-N curve for two unidirectional GF-PET laminates processed at 270 (○) and 300 °C (□), respectively (after Gauthier *et al.* [27]).

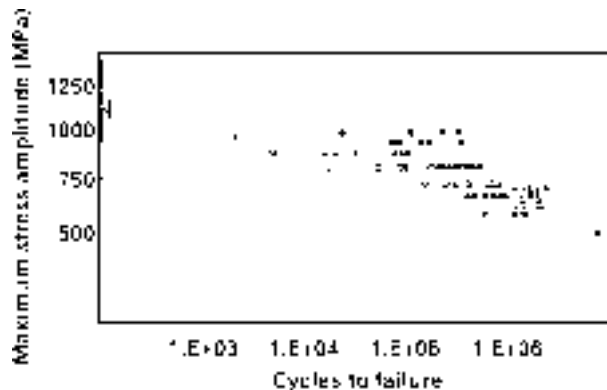


Figure 17 The tension-tension fatigue behaviour of unidirectional continuous fibre and ordered staple fibre Kevlar 49/J-2 laminates (J-2 is a polyamide copolymer; after Okine *et al.* [28]): (●) continuous, (○) discontinuous.

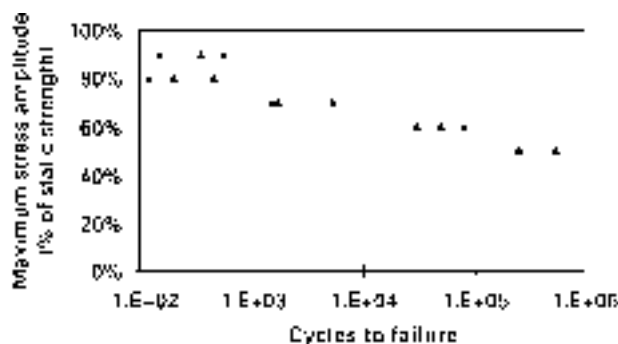


Figure 18 The S-N curve obtained for the woven material. The general trend is a gradual decrease of failure load with increasing number of load cycles. The scatter is fairly large, especially at higher load levels.

In the present work some problems were initially encountered during the fatigue testing. The specimens did, in some cases, slide sideways and lose their alignment in the three point bending jig. This was believed to be due to the fibre misalignment in the laminates. The rig was consequently modified using shallow grooves to prevent the sliding of the specimens in all subsequent tests.

These subsequent fatigue results are shown in Fig. 18. As expected, the number of load cycles increases as the maximum fatigue load decreases. At all load levels the modes and mechanisms of fatigue fracture were the same as for static fracture. The damage initiated on the compression side, usually a small distance away from the loading pin and also close to the weft bundles, as shown schematically in Fig. 19. The damage was seen to occur in the form of lines of stress whitening, which was the result of matrix cracking and crazing, Figs 20 and 21. At an increased load or at a higher number of load cycles the damage progressed out from the loading area. In the static tests this damage was accompanied by a small load drop. As the tests continued the damage finally propagated through the thickness and failure on the tensile side occurred. Tensile matrix cracking, typically as shown in Fig. 22, accumulated in the developing damage zone during the tests. Generally, however, the specimens were still able to carry a significant load after the tensile failure even though a few specimens



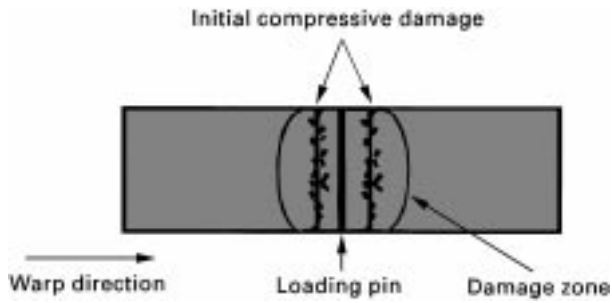


Figure 19 A schematic plan view of the compression face of a flexural fatigue specimen. The failure initiated on the compression face as compression damage just outside the loading pin, often at adjacent weft yarns. Damage then accumulated and propagated through to the tensile face and final failure occurred.

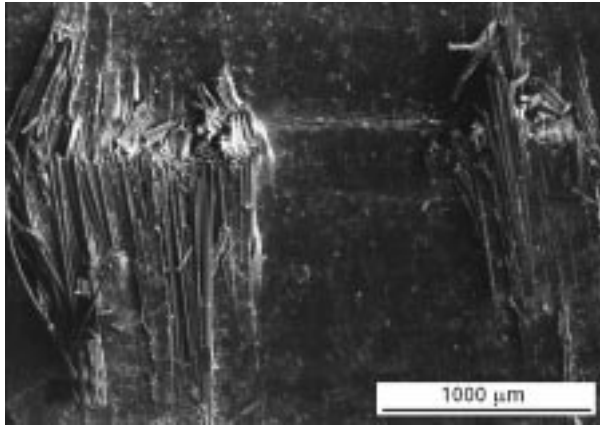


Figure 20 The compressive damage away from the loading pin on a flexural fatigue specimen. The longitudinal direction of the specimen is from the bottom to the top in the micrograph.

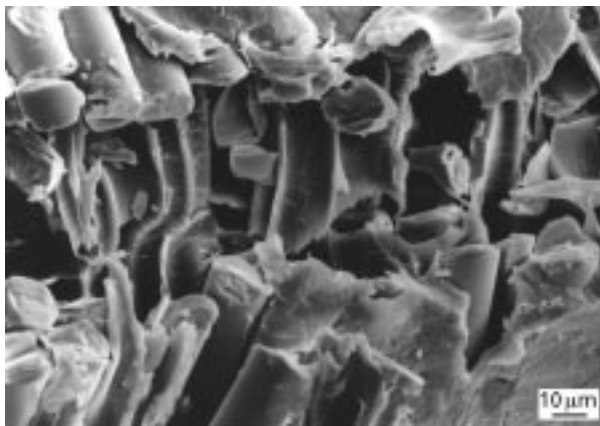


Figure 21 Close up of a compressive fibre bundle failure. The glass fibres show evidence of buckling due to the compressive loads. The longitudinal direction of the specimen is from the bottom to the top in the micrograph.

fractured catastrophically with visible fibre fractures across the full width of the tensile face. This variability in failure behaviour is not desirable from a design point of view and this tissue needs to be addressed further when manufacturing such thermoplastic textile composites.

By improving the adhesion between the fibres and the matrix the fatigue life ought to increase because crack propagation along the interface would then be more difficult. Friedrich [29] reported an improved fatigue life of injection moulded GF-PET having

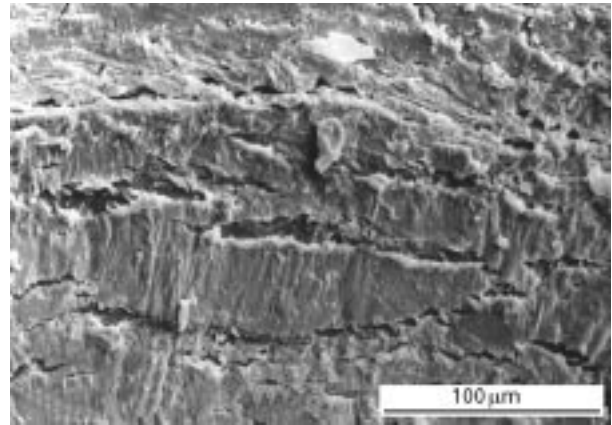


Figure 22 Cracking of the matrix, as seen in the micrograph, was one of the mechanisms that accumulated during that fatigue test. The longitudinal direction of the specimen is from the bottom to the top in the micrograph.

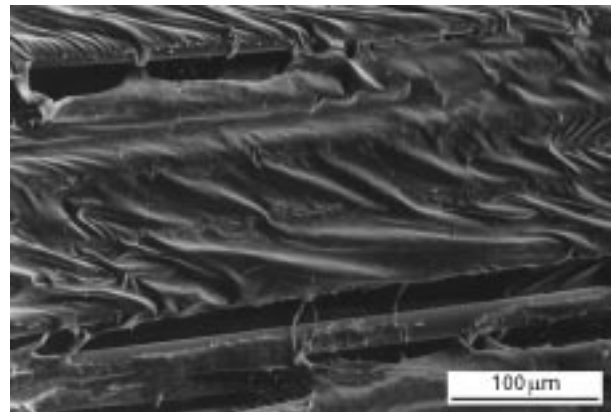


Figure 23 A wavy surface pattern was occasionally seen in the failure area on the fatigue specimens. The mechanisms for the formation of these are not fully understood.

a higher quality fibre–matrix interface. In this work Friedrich also observed that the fatigue crack growth rate was higher in areas with highly aligned fibres.

During the SEM examination of the fracture surfaces a few unusual features were seen. Fig. 23 shows a wavy matrix pattern close to the final failure. These patterns were occasionally seen in some of the specimens at different load levels and the formation of these are not fully understood. One explanation may be local plastic deformation of the matrix under the cyclic compression loading. During previous fractographic work on statically failed specimens of the same material this phenomenon was not observed. Fibrils bridging fairly large matrix cracks were also observed, Fig. 24, and this was somewhat surprising in view of the evidence of a fairly brittle matrix failure as discussed earlier.

#### 4. Conclusions

The traditional textile processes, such as weaving and warp knitting, enable a rapid production of reinforcement for structural composites. In the present work the response to mechanical loads of novel commingled unidirectional warp knitted and woven glass fibre reinforced polyethylene terephthalate (GF-PET) laminates has been characterized. The mechanical properties of the two materials were determined under



Figure 24 Fibrils bridging a matrix crack close to the location of the primary compressive damage.

tension, in-plane shear and flexure. The warp knitted material was stiffer and marginally stronger when compared to the woven material. Some manufacturing difficulties regarding, e.g. accurate fibre alignment, fibre-matrix interface quality and variability in mechanical properties, still persist.

The flexural fatigue properties were determined for the woven laminates by means of three-point bending tests with a loading ratio of  $R = 0.1$  at stress levels of 50–90% of the ultimate static strength. The laminates exhibited a decreasing failure load with an increasing number of load cycles. The decrease was similar to those previously reported in the literature for continuous fibre reinforced thermoplastic materials with a reduction to approximately 60% of the maximum static load for  $10^6$  load cycles. The failures generally initiated on the compression face and a damage zone developed from this region. An SEM examination of the specimens identified some of the mechanisms involved in failure to be tensile matrix failure, crazing, formation of wavy surface matrix features and tensile and compression glass fibre breakage.

The Mode I, Mode II and mixed mode (Mode I:II ratios 4:1, 1:1 and 1:4) interlaminar fracture toughnesses of the laminates were determined by means of the double cantilever beam and mixed mode bending (MMB) tests respectively. The initiation fracture toughnesses for the woven materials were around 1.1 and  $1.3 \text{ kJ m}^{-2}$  for Mode I and Mode II, respectively. For the warp knitted material the corresponding values were 0.9 and  $1.0 \text{ kJ m}^{-2}$ . The propagation toughnesses were up to twice as high for all materials tested.

The main fractographic features, as determined by an SEM examination, of the Mode I dominated failure were a brittle matrix failure and large amounts of fibre pull-out. As the Mode II loading component increased, the amount of fibre pull-out was reduced and the features of the matrix appeared to be more sheared. Cusps were found on the fracture surfaces of specimens tested in pure Mode II and mixed mode I:II = 1:4. Cusps are normally not found in thermoplastic matrix composites.

Both materials offer a good combination of mechanical properties and toughness and are promising for structural applications in, for example, the transportation industry.

## Acknowledgements

Financial assistance has been provided by Forbairt, The Swedish Institute, and The Marcus Wallenberg Foundation for Advanced Education in International Entrepreneurship. The assistance of Mr Martin Levesque with the flexural fatigue tests is gratefully acknowledged.

## References

1. A. G. GIBSON and J. A. MANSON, *Compos. Manufacturing* **3** (1992) 223.
2. L. YE and K. FRIEDRICH, *J. Mater. Sci.* **28** (1993) 773.
3. A. RAMASAMY and Y. WANG, *Polym. Compos.* **17** (1996) 515.
4. J. W. S. HEARLE and G. W. DU, *J. Textile Inst.* **81** (1990) 360.
5. A. B. STRONG, in "High performance and engineering thermoplastic composites" (Technomic Publishing Company, PA, 1993).
6. N. SVENSSON, R. SHISHOO and M. D. GILCHRIST, *J. Thermoplas. Compos. Mater.* **11** (1998) 22.
7. N. SVENSSON, R. SHISHOO and M. D. GILCHRIST, *Polym. Compos.* **19** (1998) in press.
8. J. H. CREWS and J. R. REEDER, *NASA TM100662* (1988).
9. J. R. REEDER and J. H. CREWS, *NASA TM102777* (1991).
10. A. J. KINLOCH, Y. WANG, J. G. WILLIAMS and P. YAYLA, *Compos. Sci. Technol.* **47** (1993) 225.
11. L. YE and K. FRIEDRICH, *Composites* **24** (1993) 557.
12. G. O. SHONAIKE, M. MATSUDA, H. HAMADA, Z. MAEKAWA and T. MATSUO, *Compos. Interfaces* **2** (1994) 157.
13. H. HAMADA, Z.-I. MAEKAWA, N. IKEGAWA, T. MATSUO and M. YAMANE, *Polym. Compos.* **14** (1993) 308.
14. N. S. CHOI, H. YAMAGUCHI and K. TAKAHASHI, *J. Compos. Mater.* **30** (1996) 760.
15. J. JANG and H. KIM, *Polym. Compos.* **18** (1997) 125.
16. W. BRADLEY, C. CORLETO and M. HENRIKSEN, in Proceedings of Sixth International Conference on Composite Materials (ICCM-VI) London, edited by F. L. Matthews, N. C. R. Buskell, J. M. Hodgkinson, and J. Morton (Elsevier, London, 1987) p. 3378.
17. T. JOHANNESSON and M. BLIKSTAD, in ASTM STP 876 (American Society for Testing and Materials, PA, 1985) p. 411.
18. T. JOHANNESSON, P. SJÖBLOM and R. SELDÉN, *J. Mater. Sci.* **19** (1984) 1171.
19. L. ARCAN, M. ARCAN and I. M. DANIEL, in ASTM STP 948 (American Society for Testing and Materials, PA, 1987) p. 41.
20. M. L. BENZEGGAGH and M. KENANE, *Compos. Sci. Technol.* **56** (1996) 439.
21. N. SVENSSON and M. D. GILCHRIST, *Mech. of Compos. Mater. & Struct.* **5** (1998) 291.
22. M. R. PIGGOT, *Compos. Sci. Technol.* **55** (1995) 269.
23. S. L. DONALDSON, *Composites* **16** (1985) 103.
24. A. BEEHAG and L. YE, **27A** (1996) 175.
25. M. D. GILCHRIST and N. SVENSSON, *Compos. Sci. Technol.* **55** (1995) 195.
26. L. HOFFMANN and S. S. WANG, *Eng. Fracture Mech.* **52** (1995) 1151.
27. M. GAUTHIER, J. CHAUCHARD, B. CHABERT and J. P. TROTIGNON, *Die Angewandte Makromolekulare Chemie* **221** (1994) 137.
28. R. K. OKINE, D. H. EDISON and N. K. LITTLE, *J. Reinforced Plastics Compos.* **8** (1990) 70.
29. K. FRIEDRICH, *Plastics and Rubber Processing and Applications* **3** (1983) 255.

Received 16 December 1997  
and accepted 11 May 1998